Voltammetry under High Mass Transport Conditions. The High-Speed Channel Electrode and Transient Measurements

Francisco Prieto, W. Joanne Aixill, John A. Alden, Barry A. Coles, and Richard G. Compton*

Physical and Theoretical Chemistry Laboratory, Oxford University, South Parks Road, Oxford OX1 3QZ, United Kingdom

Received: January 23, 1997; In Final Form: April 27, 1997[⊗]

The application of the high-speed channel microband electrode to potential step transient measurements is reported. Potential step experiments, from conditions of no current flows up to a potential value where the mass transport limited current is reached, using the one-electron oxidation of *N*,*N*,*N*′,*N*′-tetramethyl-1,4-phenylendiamine and the one-electron reduction of *p*-bromonitrobenzene and *p*-chloronitrobenzene are reported. The applicability of a model in which the dominant mass transport form is by diffusion normal to the electrode and by convection axially through the channel is demonstrated so that axial diffusion effects are negligible. This permits the use of the backward implicit procedure to analyze the experimental transient responses incorporating any kinetic complications, as appropriate. It is shown that homogeneous rate constants of at least 1 order of magnitude higher are accessible by potential step transient measurements for an ECE mechanism as compared to steady-state experiments.

Introduction

During the last 15 years much effort has been made to reduce the time scale accessible in electrochemical experiments, through the enhancement of the mass transport to the electrode. In particular the introduction of microelectrodes,[1−3] with at least one dimension of only a few micrometers or less in size, has significantly extended the voltammetric time scale[4]. The rate of mass transport to such electrodes is much higher than to electrodes of conventional size, allowing the study of kinetic processes, either heterogeneous or homogeneous, that were previously masked by the mass transport control. The use of microelectrodes for kinetic measurements has been recently reviewed,[3] showing that the dependence of the steady-state electrode current on the electrode size can provide kinetic data. Specifically, the voltammetric response under steady-state conditions over microdisc electrodes can be applied to study reactions with rate constant values of the same order as the ratio D/a^2, where D is the diffusion coefficient and a the radius of the microdisc;[5] when using a microdisc electrode with radii of ~ 1 μm, processes with first-order rate constants in the range 10^2-10^4 s^{-1} are accessible.[3] These values can be significantly improved upon by the use of transient methods. In particular the use of fast scan cyclic voltammetry ($\leq 10^6$ V s^{-1}) in combination with microelectrodes has demonstrated the feasibility of approaching the nanosecond time scale.[4,6,7]

Recently, the voltammetric time scale accessible by *steady-state* measurements has been significantly extended through the enhancement of mass transport to microelectrodes using forced convection in addition to diffusion,[8−14] allowing the investigation of faster homogeneous and heterogeneous processes. First, Macpherson, Marcar, and Unwin[11] have introduced an elegant wall-tube microelectrode in which a narrow fluid jet impinges uniformly over a microdisc electrode. Secondly, Compton and co-workers[12] have reported a fast flow channel electrode in which solution is pumped at high speed ($\leq$150 miles/h) over a microband electrode of length 1−50 μm, so as to realize a mass transport coefficient of ca. 1 cm s^{-1}.

The high-speed channel electrode (HSCE) has been applied to the study of homogeneous chemical processes coupled to electron transfer reactions[12] and heterogeneous electron transfer.[13] It was shown from steady-state voltammetric experiments that homogeneous first-order rate constants[12] as high as 10^4-10^5 s^{-1} and standard electrochemical rate constants[13] as high as ca.1 cm s^{-1} were readily measurable. The purpose of this paper is to extend the application of the HSCE to potential step transient measurements. The necessary theory is summarized in the next section, and in particular, the role, if any, of axial diffusion is explored.

Theory

The aim of this section is to establish the form of the current−time curves expected for potential step transients at the HSCE in the case of a reversible electron transfer of the form

$$A \pm e^- \rightleftarrows B$$

where the bulk solution only contains A. The transients are those for potential steps from no current to the transport-limited value (regardless of the electrode kinetics).

The dimensions and coordinates of the channel electrode are depicted in Figure 1. of ref 12. With reference to the coordinate system shown, the corresponding time-dependent mass transport equation is

$$\frac{\partial a}{\partial t} = D\frac{\partial^2 a}{\partial x^2} + D\frac{\partial^2 a}{\partial y^2} - v_x\frac{\partial a}{\partial x} \qquad (1)$$

where a is the concentration of species A, D is its diffusion coefficient, and v_x is the x velocity component of the flow. In eq 1 it has been assumed that the diffusion is negligible in the z direction. Provided the solution flow is laminar and fully

* To whom correspondence should be addressed.
[⊗] Abstract published in *Advance ACS Abstracts,* June 15, 1997.

S1089-5647(97)00307-6 CCC: $14.00

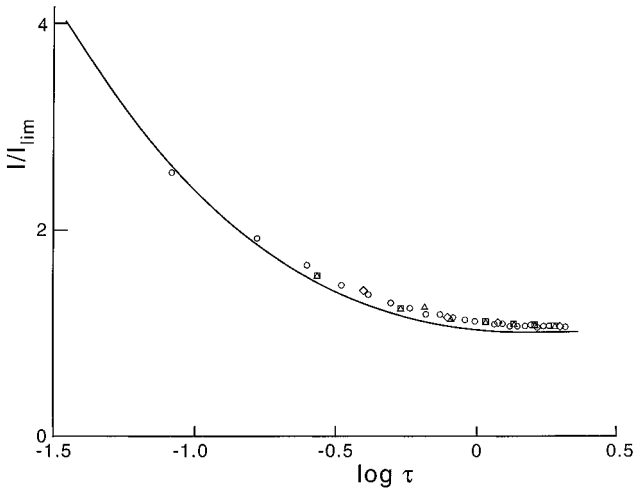

Figure 1. Working curve for normalized transients (—) and experimental normalized transients for pCNB at four different flow rates: 0.1429 $cm^3\ s^{-1}$ (○), 0.8448 $cm^3\ s^{-1}$ (□), 1.5044 $cm^3\ s^{-1}$ (△), and 0.3367 $cm^3\ s^{-1}$ (◇).

developed in the vicinity of the electrode, v_x is a parabolic function of the y coordinate:[15]

$$v_x = v_0\left[1 - \frac{(h-y)^2}{h^2}\right] \tag{2}$$

where h is the half-height of the channel and v_0 is the velocity at the center of the channel (when $y = h$) in the x direction:

$$v_0 = \frac{3}{4}\frac{v_f}{hd} \tag{3}$$

with v_f being the solution flow and d the width of the channel.

The boundary conditions defining the potential step problem specified above are

$$t < 0, \quad \text{all } x, \quad \text{all } y, \quad [A] = [A]_{bulk}$$

$$t \geq 0, \quad y = 0, \quad 0 < x < x_e, \quad [A] = 0$$

$$\text{all } t, \quad y = 2h, \quad \text{all } x, \quad \frac{\partial[A]}{\partial y} = 0$$

where x_e is the length of the microband (see Figure 1) and $[A]_{bulk}$ is the bulk concentration of A.

A rigorous solution of eq 1 has been obtained by Bidwell et al.[15] for potential step transients at channel microband electrodes, based on the strongly implicit procedure (SIP), which permits the numerical solution of eq 1. It was shown that these transients when normalized to their steady-state value in the absence of axial diffusion as predicted by the Levich equation,[16]

$$I_{lim,Lev} = 0.925Fw[A]_{bulk}x_e^{2/3}D^{2/3}(V_f/h^2d)^{1/3} \tag{4}$$

where F is the Faraday constant, are a unique function, f, of two dimensionless parameters, p and τ, so that

$$\frac{I}{I_{lim,Lev}} = f(p,\tau) \tag{5}$$

It must be noted that eq 5 assumes the Lévêque approximation,[17] in which the convective flow profile is assumed to be linear instead of parabolic in the vicinity of the electrode.

The definitions of p and τ are

$$p = \left(\frac{Dh}{2v_0x_e^2}\right)^{2/3} \tag{6}$$

$$\tau = t\left(\frac{4v_0^2D}{h^2x_e^2}\right)^{1/3} \tag{7}$$

Therefore, the complete working surface, given in ref 15 as a contour plot of $I/I_{lim,Lev}$ against $\log(p)$ and $\log(\tau)$, can be used for the analysis of data recorded at any flow rate or cell geometry, including cases in which the axial diffusion effects are significant. In this latter case the steady-state current also deviates from that predicted by eq 4.

It can be noted that the parameter p in the complete working surface gives an estimation of the axial diffusion contribution to the mass transport;[15] thus higher p values imply more significant axial diffusion effects, so the relative contribution of the axial diffusion component of the mass transport decreases when the solution flow rate increases. It follows that it might be the case that axial diffusion effects at the HSCE can be neglected in transient measurements, in the same way as they are in steady-state measurements where the Levich equation holds.[12] In this case the relevant mass transport along the x coordinate includes only the convective term, and eq 1 can be simplified to

$$\frac{\partial a}{\partial t} = D\frac{\partial^2 a}{\partial y^2} - v_x\frac{\partial a}{\partial x} \tag{8}$$

The aim of this paper is to examine experimentally whether the neglect of axial diffusion under transient—as opposed to steady-state—conditions is justified.

Equation 8 can be solved numerically using the procedure developed by Fisher et al.[18] based on the backward implicit (BI) method introduced by Anderson[19] for the simulation of channel electrode problems. In these cases the normalized transient current with respect to the transport limiting current, $I_{lim,Lev}$, is solely a unique function of the normalized time, τ, defined by eq 6. Therefore, under conditions in which the axial diffusion effects can be neglected the chronoamperometric data can be analyzed using the unique working curve given in Figure 1. Note that the simulation data in Figure 1 are consistent with the approximate analytical theory of Aoki.[20]

Experimental Section

The fast flow channel electrode system has been described in previous papers[12−14] and consists basically of a pressurized system used to force solutions to flow through the channel cell.

This cell is constructed from fused blocks of silica (Optiglass Ltd., Hainault, Essex, U.K.) and is designed to very rapidly accelerate the flow by a factor of 35, as it enters in the channel through a taper section. The upstream length of the channel is 2 mm to ensure that a laminar flow regime is established in the vicinity of the microband electrode. The section of the channel is 2 mm (width) × 0.1 mm (height).

The channel flow cell is completed by a cover plate which contains the Pt microband electrode used in the experiments reported here. It was made by a metal−glass sealing procedure in order to avoid the use of adhesives that would restrict the number of solvents amenable to study. A platinum foil strip (Goodfellow Metals, Cambridge, U.K., 99.95% purity) was sandwiched between two 9 mm diameter Pyrex rods, and the junction heated until the assembly fused. A free tail of Pt foil was left to protrude from one side and was soldered to a copper clip attached to the glass with Araldite epoxy resin in order to make the electrical contact to the potentiostat. The section of

glass carrying the electrode was then cut out and ground to a rectangular shape using standard glass-working diamond tools. This was then lapped to a flat surface and polished using a sequence of silicon carbide and alumina abrasives, decreasing the particle sizes to 0.3 μm. The last steps of the polishing procedure were repeated after every experiment. A Topometrix atomic force microscope was used to ensure that the lapping and polishing procedure did not cause undercutting of the electrode and to measure the precise dimensions of it: 40.6 μm length (x_e) and 0.94 mm width (w).

The three-electrode cell was completed with a Pt auxiliary electrode located downstream of the working electrode, in order to avoid interferences with the reaction products of the counter electrode; as reference electrode, a Pt wire was located upstream of the channel. The potential of this pseudoreference electrode was regularly calibrated with steady-state experiments employing the oxidation of ferrocene. All the experiments, either steady-state voltammograms or potential step transients, were performed using a "home-built" potentiostat controlled by the same PC computer as the pressurized system.

The solvent used throughout was freshly dried acetonitrile (Fisons, dried, distilled); the background electrolyte was tetrabutylammonium perchlorate (TBAP, Kodak, puriss), 0.1 M. Ferrocene (Cp_2Fe), *N*,*N*,*N*′,*N*′-tetramethyl-1,4-phenylenediamine (TMPD), *p*-bromonitrobenzene, (pBNB), and *p*-chloronitrobenzene (all Aldrich, 99%) were used as received. Solutions were thoroughly purged of oxygen with predried nitrogen; special care was taken with TMPD solutions, in which the solvent was previously purged of oxygen, in order to avoid the oxidation of TMPD solutions.

All the theoretical data were generated using the supporting programs written in FORTRAN 77 on a Convex 220.

Results and Discussion

In order to calibrate the height of the channel steady-state experiments on the oxidation of 0.5 mM Cp_2Fe in 0.1 M TBAP/acetonitrile, a well-established simple one-electron process[21] was carried out. The half-wave potential measured was $+0.225 \pm 0.01$ (V vs Pt pseudoreference electrode) for different electrolyte flow rates, up to 3.5 cm^3 s^{-1}. The mass transport limited current showed a linear dependence on the cube root of the flow rate according to the Levich equation, eq 4. The introduction in eq 4 of the measured geometric parameters of the channel electrode (x_e, w, and d), given in the Experimental Section, and a value of 2.3×10^{-5} cm^2 s^{-1} for the diffusion coefficient of Cp_2Fe in acetonitrile, according to the literature,[21] permitted us to obtain the height of the channel. In all cases a value of 95 ± 7 μm was found.

Similar steady-state voltammetric experiments were recorded using 0.5 mM solutions of TMPD, pBNB, and pCNB in 0.1 M TBAP/acetonitrile. In all cases electrochemically reversible one-electron voltammetric waves were obtained, with half-wave potentials of ca. +0.185, −1.390, and −1.230 (V vs Pt pseudoreference electrode) for the oxidation of TMPD and the reductions of pBNB and pCNB, respectively. The mass transport limited current dependence on the electrolyte flow rate was in excellent agreement with the behavior predicted by the Levich equation, eq 4, as can be seen in Figure 2a−c. The diffusion coefficient of each electroactive species used was obtained from the slopes of the linear plots in Figure 2a−c and the channel geometric parameters obtained previously. The D values obtained for TMPD, pBNB, and pCNB were 2.15, 2.3, and 2.05 ($\times 10^5$ cm^2 s^{-1}; $\pm$10%), respectively.

Note here that the basis of the Levich equation is that the dominant forms of mass transport are convection axially through the cell and diffusion normal to the electrode surface, so the axial diffusion contribution to the overall mass transport is neglected. The agreement between the experimental data and the Levich equation demonstrates the nonexistence of axial diffusion effects in the steady-state measurements under the experimental conditions used in the high-speed channel electrode.

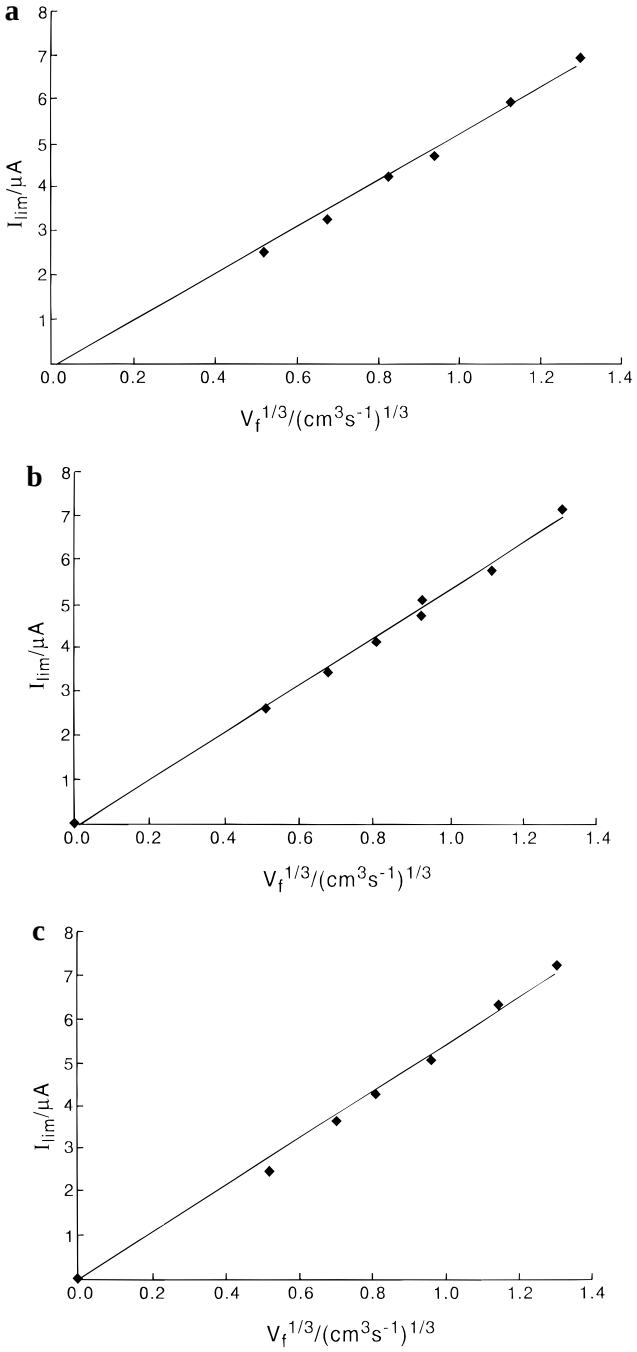

Figure 2. (a) Transport limited current (I_{lim})/flow rate (v_f) data obtained for the oxidation of TMPD (0.5 mM) in 0.1 M TBAP/acetonitrile solution. (b) Transport limited current (I_{lim})/flow rate (v_f) data obtained for the reduction of pBNB (0.5 mM) in 0.1 M TBAP/acetonitrile solution. (c) Transport limited current (I_{lim})/flow rate (v_f) data obtained for the reduction of pCNB (0.5 mM) in 0.1 M TBAP/acetonitrile solution.

Potential step experiments were performed at different flow rates for each of the three chemical systems of interest. The steps were made from an initial potential at the bottom of the voltammetric wave where no appreciable current flowed, up to a potential at the top of the wave where the mass transport

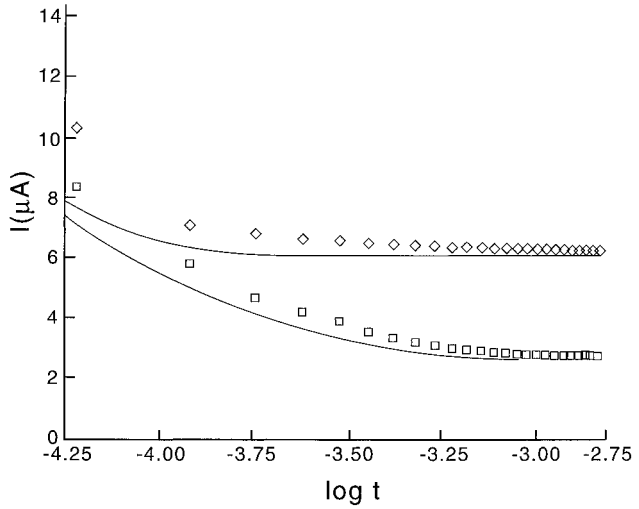

Figure 3. Current−time transients recorded using 0.5 mM TMPD in 0.1 M TBAP/acetonitrile solution at a flow rate of 1.406 $cm^3\ s^{-1}$ (◇) and 0.5 mM pBNB in 0.1 TBAP/acetonitrile solution at a flow rate of 0.1418 $cm^3\ s^{-1}$ (□). The solid line represents the theoretically predicted transient as calculated using BI.

limited current was reached. The corresponding transient current recorded as a function of the time showed an extremely fast decay, faster at higher flow rates, as shown in Figure 3. In all cases 99% of the steady-state response was reached in less than 1 ms and about 0.1 ms for the higher flow rates.

The experimental data were analyzed using the BI method[18] conforming to eq 8. Good agreement between experimental data and the simulated values without considering the axial diffusion effect was obtained in all the conditions investigated, as can be seen in Figure 3. These observations suggest that the axial diffusion effect can be neglected in transient experiments using the HSCE. As was mentioned above, under the experimental conditions used in the HSCE and if the Lévêque approximation holds,[17] the normalized transient current with respect to the steady-state value predicted by the Levich equation is a unique function of the dimensionless time parameter, τ (eq 7), and the experimental data can be analyzed using the simple working curve given in Figure 1. In the same figure some experimental results at different flow rates are plotted. The experimental agreement found with the working curve generated by the BI method indicates once more the validity of the assumption of nonaxial diffusion effects in HSCE transient experiments.

The p values calculated using eq 6 and the geometrical and flow parameters corresponding to the HSCE are lower than 1×10^{-3}. In the complete working surface in ref 15 it can be seen that for such low p values the transient response does not depends on the p value; it is a unique function of the dimensionless time parameter, τ, as must be expected if axial diffusion effects are negligible.

An additional check of the axial diffusion effect was made through the comparison of the transient current simulated by the BI method according to eq 8, and those obtained with the SIP following the complete eq 1, for the less favorable case, at one of the lower flow rates achieved with the fast flow system, where the relative effect of the axial diffusion in the overall mass transport was higher. The results for the geometric parameters of the HSCE given in the Experimental Section are shown in Figure 4. The differences between the values predicted by both methods are negligible, as was expected. This clearly demonstrates the validity of the assumption of no axial diffusion effect on the mass transport for transient experiments in the HSCE.

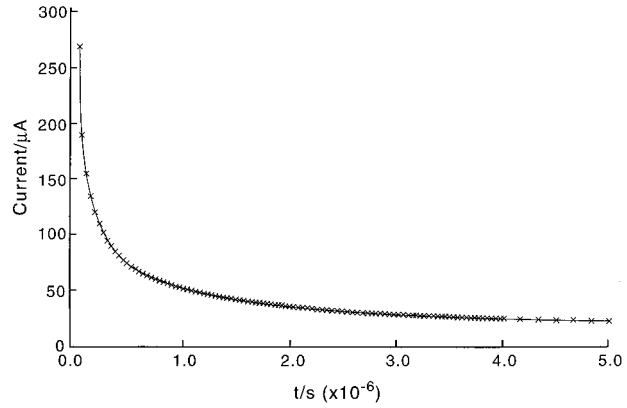

Figure 4. Current−time transients simulated for a 40.6 μm electrode using BI which does not include axial diffusion effects (—) and SIP where axial diffusion effects are taken in to account, (×).

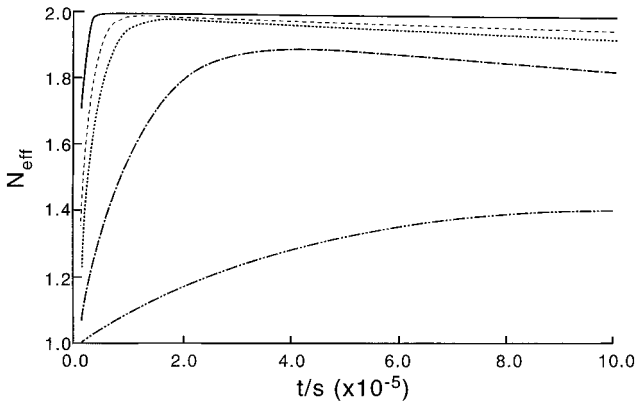

Figure 5. Number of effective of electrons vs time corresponding to an ECE mechanism at a 40 μm electrode calculated using BI and the values for the homogeneous rate constant: $10^7\ s^{-1}$ (—), $10^6\ s^{-1}$ (- - -), $5 \times 10^5\ s^{-1}$ (•••), $10^5\ s^{-1}$ (-•-), and $1 \times 10^4\ s^{-1}$ (-••-).

Therefore, the BI procedure is an appropriate method to analyze the transient current data obtained with the fast flow system, with the advantages that this fact represents mainly that changes in mechanism are readily incorporated, so the HSCE can be used in combination with the BI procedure to investigate through potential steps measurements mechanistic problems that change the transient current response (CE, EC′, ECE, ...), providing a powerful tool to access higher rate constants. An example of this is given in Figure 5, in which the effective number of electrons corresponding to the transient response of a system following an ECE mechanism at a 40 μm band is plotted vs the time. It can be seen that provided current−time transients can be experimentally recorded on the microsecond time scale, then homogeneous rate constants of ca. $1 \times 10^6\ s^{-1}$ are accessible with transient experiments, 1 order of magnitude higher than that corresponding to a steady-state experiment, $1 \times 10^5\ s^{-1}$. The reduction of the electrode length to dimensions ~1 μm should reduce the time scale by a further order of magnitude.

Acknowledgment. We thank the EC for financial support (Grant No. ERBFMBICT950219) for F.P. and the EPSRC for studentship for J.A.A. and W.J.A. J.A.A. also thanks Keble College, Oxford, for a Senior Scholarship.

References and Notes

(1) Fleischmann, M.; Pons, S. *Ultramicroelectrodes*; Datatech: Morgantown, NC, 1987.
(2) Wang, J. *Microelectrodes*; VCH: New York, 1990.
(3) Montenegro, M. I. *Res. Chem. Kinet.* **1994**, *2*, 1.

(4) Burlatsky, S. F.; Reindhart, W. P. *J. Phys. Chem* **1995**, *99*, 5518.
(5) Oldham, K. B. *J. Electroanal. Chem.* **1991**, *313*, 3.
(6) Amatore, C.; Lefrou, C. *Port. Electrochim. Acta* **1991**, *9*, 311.
(7) Amatore, C.; Jutand, A.; Pfluger, F. *J. Electroanal. Chem.* **1987**, *218*, 361.
(8) Compton, R. G.; Fisher, A. C.; Wellington, R. G.; Dobson, P. J.; Leigh, P. A. *J. Phys. Chem.* **1993**, *97*, 10410.
(9) Compton, R. G.; Wellington, R. G.; Dobson, P. J.; Leigh, P. A. *J. Electroanal. Chem.* **1994**, *370*, 129.
(10) Compton, R. G.; Dryfe, R. A. W.; Alden, J. A.; Rees, N. V.; Dobson, P. J.; Leigh, P. A. *J. Phys. Chem.* **1994**, *98*, 1270.
(11) Macpherson, J. V.; Marcar, S.; Unwin, P. R. *Anal. Chem.* **1994**, *66*, 2175. Macpherson, J. V.; Beeston, M. A.; Unwin, P. R. *J. Chem. Soc., Faraday Trans.* **1995**, *91*, 899.
(12) Rees, N. V.; Dryfe, R. A. W.; Cooper, J. A.; Coles, B. A.; Compton, R. G. *J. Phys. Chem.* **1995**, *99*, 7096.
(13) Rees, N. V.; Alden, J. A.; Dryfe, R. A. W.; Coles, B. A.; Compton, R. G. *J. Phys. Chem.* **1995**, *99*, 14813.
(14) Coles, B. A.; Dryfe, R. A. W.; Rees, N. V.; Compton, R. G.; Davies, S. G.; McCarthy, T. D. *J. Electroanal. Chem.* **1996**, *411*, 121.
(15) Bidwell, M. J.; Alden, J. A.; Compton, R. G. *J. Electroanal. Chem.* **1996**, *414*, 247.
(16) Levich, V. G. *Physicochemical Hydrodynamics*; Prentice-Hall: Englewood Cliffs, NJ, 1962.
(17) Lévêque, M. A. *Ann. Mines. Mem. Ser.* **1928**, *12/13*, 201.
(18) Fisher, A. C.; Compton, R. G. *J. Phys. Chem.* **1991**, *95*, 7538.
(19) Anderson, J. L.; Moldoveanu, S. *J. Electroanal. Chem.* **1984**, *179*, 107.
(20) Aoki, K.; Tokuda, K.; Matsuda, H. J. *J. Electroanal. Chem.* **1987**, *217*, 33.
(21) Sharp, P. *Electrochim. Acta* **1983**, *28*, 301. Schull, H.; Sochaj, K. *Electrochim. Acta* **1989**, *34*, 915.